International Journal of Remote Sensing, 2013
Vol. 34, No. 24, 8789–8802, http://dx.doi.org/10.1080/01431161.2013.853143

Taylor & Francis
Taylor & Francis Group

Using hyperspectral vegetation indices to estimate the fraction of photosynthetically active radiation absorbed by corn canopies

Changwei Tan[a]*, Arindam Samanta[b], Xiuliang Jin[a], Lu Tong[a], Chang Ma[a], Wenshan Guo[a], Yuri Knyazikhin[c], and Ranga B. Myneni[c†]

[a]*Key Laboratory of Crop Genetics and Physiology of Jiangsu Province, College of Agriculture, Yangzhou University, Yangzhou 225009, PR China;* [b]*Atmospheric and Environmental Research, Lexington, MA 02421, USA;* [c]*Department of Geography and Environment, Boston University, Boston, MA 02215, USA*

(*Received 21 December 2012; accepted 8 May 2013*)

The fraction of photosynthetically active radiation (FPAR) absorbed by vegetation – a key parameter in crop biomass and yields as well as net primary productivity models – is critical to guiding crop management activities. However, accurate and reliable estimation of FPAR is often hindered by a paucity of good field-based spectral data, especially for corn crops. Here, we investigate the relationships between the FPAR of corn (*Zea mays* L.) canopies and vegetation indices (VIs) derived from concurrent *in situ* hyperspectral measurements in order to develop accurate FPAR estimates. FPAR is most strongly (positively) correlated to the green normalized difference vegetation index (GNDVI) and the scaled normalized difference vegetation index (NDVI*). Both GNDVI and NDVI* increase with FPAR, but GNDVI values stagnate as FPAR values increase beyond 0.75, as previously reported according to the saturation of VIs – such as NDVI – in high biomass areas, which is a major limitation of FPAR-VI models. However, NDVI* shows a declining trend when FPAR values are greater than 0.75. This peculiar VI–FPAR relationship is used to create a piecewise FPAR regression model – the regressor variable is GNDVI for FPAR values less than 0.75, and NDVI* for FPAR values greater than 0.75. Our analysis of model performance shows that the estimation accuracy is higher, by as much as 14%, compared with FPAR prediction models using a single VI. In conclusion, this study highlights the feasibility of utilizing VIs (GNDVI and NDVI*) derived from ground-based spectral data to estimate corn canopy FPAR, using an FPAR estimation model that overcomes limitations imposed by VI saturation at high FPAR values (i.e. in dense vegetation).

1. Introduction

The fraction of incoming solar radiation (400−700 nm spectral range) absorbed by green vegetation canopies (Moreau and Li 1996; Ma et al. 2007) – known as the fraction of photosynthetically active radiation (FPAR) absorbed by vegetation – is critical to understanding and quantifying the exchange of energy, mass, and momentum between the land surface and the atmosphere, and thus a key state variable in much of ecosystem productivity (including crop biomass models (Wu et al. 2010) and climate models (e.g. Sellers et al. 1997)). As a measure of the photosynthetic capacity of plant canopies and, therefore, being linked to plant productivity, FPAR can be used for guiding crop cultivation

†Corresponding author. Email: ranga.myneni@gmail.com
*Present address: Agricultural College, Yangzhou University, 48 Wenui Road (E), Yangzhou 225009, Jiangsu Province, PR China.

activities (Daughtry et al. 1992). However, conventional methods of FPAR estimation from field observations, which often involve complicated site-specific parameterizations and calculations, make it difficult to apply over large agricultural areas. These shortcomings can be overcome through the complementary use of hyperspectral measurements of crops, which have several advantages – they are non-destructive, uniform, can be performed rapidly, and no complicated parameterizations are necessary.

Estimation of FPAR from vegetation indices (VIs) derived from hyperspectral data, especially remote-sensing data, has been reported by several studies (Ruimy and Saugier 1994; Fensholt, Sandholt, and Rasmussen 2004; Gobron et al. 2006; Olofsson and Eklundh 2007; Zhao et al. 2009; Chiesi et al. 2011). For instance, Eduardo, Jose, and Minguez (1998) compared the performance of VIs to estimate FPAR of legume crops and concluded that, of the nine types of VI having a close relationship with FPAR, the modified soil-adjusted vegetation index (MSAVI) performed best. Roujean and Breon (1995) reported an approximately linear relationship between the difference vegetation index (DVI) and FPAR for low ground cover. On the other hand, if ground cover is significant, the impact of background significantly reduces and FPAR could be better estimated using the normalized difference vegetation index (NDVI). The re-normalized difference vegetation index (RDVI) showed an approximately linear relation to FPAR regardless of ground cover. Chen (1996a, 1996b) found that the simple ratio (SR) and NDVI were better correlated with *in situ*-measured FPAR compared with other VIs in Canadian boreal forests. The VI–FPAR relationship in boreal forests differed significantly from that in non-forested ecosystems due to the impact of background signals and changes in canopy architecture. Daughtry et al. (1992) compared the spectral characteristics of soybean and corn canopies and concluded that there was a significant non-linear relationship between FPAR and VIs. Friedl et al. (1995) observed that in the absence of constraints imposed by soil, water, and mineral nutrients, FPAR was directly proportional to the growth rate of the canopy and was also approximately linearly related to NDVI. Goward et al. (1994) confirmed a strong linear relationship (R^2 = 0.99) between the Advanced Very High Resolution Radiometer (AVHRR) NDVI and *in situ*-measured FPAR for forested trees. However, the regression analysis was based on only five points, making it statistically uncertain. Other studies using radiative transfer models (Goward and Huemmrich 1992; Myneni and Williams 1994; Moreau and Li 1996; Olofsson and Eklundh 2007) showed evidence of a linear relationship, or the use of linear models, and concluded that NDVI generally performs well at estimating FPAR.

Modelled FPAR products based on MODIS have recently been reported in several studies. Coops et al. (2011) investigated the increasing availability of time series of FPAR data from MODIS and indicated that the three dynamic habitat index components varied significantly in their magnitude, principally because of MODIS FPAR estimates being larger than those observed by Medium Resolution Imaging Spectrometer (MERIS) FPAR. Turner et al. (2005) compared MODIS FPAR to measurements for sites in the USA and found the product to overestimate ground-measured FPAR. Senna, Costa, and Shimabukuro (2005) compared the FPAR from MODIS with *in situ* measurements for a tropical rainforest in Brazil and concluded that the MODIS FPAR was reliable for FPAR estimation. There is a need for investigation of the performance of VIs in different vegetation ecosystems (Olofsson and Eklundh 2007).

Models based on linear FPAR–NDVI relationships suffer from a major flaw – NDVI saturates at high leaf area index values (~3.5, see for example Samanta et al. 2012), and thus a linear model tends to be insensitive to FPAR changes in such cases (Myneni and Williams 1994; Olofsson and Eklundh 2007). Another issue that needs to be recognized is

the scarcity of data for boreal ecosystems. The majority of the studies cited above present empirical evidence suggesting a functional relationship between FPAR and spectral VIs, and these are mostly focused on forests, grasses (prairies), and some crop types such as rice, wheat, and cotton (Hall et al. 1992; Fensholt, Sandholt, and Rasmussen 2004). There are only a few reports (Ren et al. 2006; Yang et al. 2007) on quantitative estimation of FPAR for corn canopies using VI from remote-sensing data. Besides, VI–FPAR relationships differ from one ecosystem type to another due to the influences of vegetation type, strong background signals, canopy structure, and spatial heterogeneity (Chen 1996). Furthermore, existing remote-sensing-based FPAR products lack adequate ground validation, which is critical to establishing the uncertainty and accuracy of such products so that they can be used for guiding crop production practices (Wu, Zeng, and Huang 2004).

This study is motivated by the above-mentioned issues and focuses on exhaustive statistical analyses of FPAR–VI relationships for corn canopies using hyperspectral data collected from a series of field experiments, and aims at determining a practical methodology for estimating FPAR of corn canopies.

2. Materials and methods

2.1. Experimental design

Three varieties of corn (*Zea mays* L.) – Nonghua No. 8, Jinhai No. 5, and Zhengdan 958 – were used in field experiments conducted during July–September of 2009−2011 at the campus experimental farm of Yangzhou University, China (119° 18′ E, 32° 26′ N). These, preceded by wheat, were planted in yellow–brown soil (Alfisols in US taxonomy) with 2.23% organic matter, 115.3 mg kg^{-1} available nitrogen, 23.8 mg kg^{-1} available phosphorus, and 78.6 mg kg^{-1} available potassium in the 0−30 cm layer of soil. Canopy spectral measurements were made alongside quasi-simultaneous measurements of photosynthetically active radiation (PAR) incident upon the growing corn canopies. In order to highlight variations in corn growth due to biochemical composition changes, three different levels of nitrogen fertilization were implemented – non-nitrogen fertilization (N_0), adequate nitrogen fertilization (N_1: N 450 kg ha^{-1}), and heavy nitrogen fertilization (N_2: N 900 kg ha^{-1}). The repeat rate of every nitrogen level was three times. Row spacing was 70 cm and plant spacing was 60 cm. The plot area was 20 m × 20 m. Local standard corn cropping management practices pertaining to water, pests, diseases, and weeds were followed. Training data consisted of 76 samples from 2009, and test data comprised 60 samples from 2010 and 2011.

2.2. Measurements and data analysis

2.2.1. Canopy hyperspectral reflectance data

In 2009, seven spectral measurements were carried out at the corn-jointing stage (19 July), little bell stage (28 July), big bell stage (6 August), booting stage (11 August), pre-silking stage (20 August), mid-silking stage (29 August), and milk stage (5 September). All canopy spectrometry determinations were taken from a vertical height to a canopy of 1.6 m, under cloudless or near-cloudless conditions between 11:00 and 14:00 Beijing Time, using an ASD FieldspecPro spectrometer (Analytical Spectral Devices, Boulder, CO, USA) fitted with 25° field-of-view fibre optics, operating in the 350−2500 nm spectral region with a sampling interval of 1.4 nm between 350 and 1050 nm, and 2 nm between l050 and 2500 nm, and with a spectral resolution of 3 nm at 700 nm,

10 nm at 1400 nm, selecting representative, growth-uniform, pest-free plants and angling the probe of the sensor downward while measuring. A 40 cm × 40 cm $BaSO_4$ calibration panel was used for calculation of hyperspectral reflectance. Vegetation and panel radiance measurements were taken by averaging 20 scans at an optimized integration time, with a dark current correction at each spectrometry determination.

In 2010, three spectral measurements with 40 test samples were carried out at the corn-jointing stage (23 July), big bell stage (7 August), and mid-silking stage (29 August). The other measurements were the same as those taken in 2009.

In 2011, two spectral measurements with 20 test samples were carried out at the corn little bell stage (July 26) and booting stage (August 13). The other measurements were the same as those taken in 2009.

2.2.2. *Spectral smoothing*

A spectral smoothing process was performed in order to remove high-frequency noise and random errors caused by spectral measuring instruments, which enhanced signal-to-noise ratio. A five-point weighted smoothing method, as reported by Smith, Steven, and Colls (2004), was used to process the raw spectral data. The five-point weighted smoothing method is carried out in the following equation:

$$n = \left(\frac{m_{-2}}{4} + \frac{m_{-1}}{2} + \frac{m}{1} + \frac{m_1}{2} + \frac{m_2}{4}\right) \Big/ 25, \tag{1}$$

where n is the weighted average of the intermediate data points in the filter window, namely the smoothed spectrum value, and m is the value of unsmoothed data points, namely the original spectral value.

2.2.3. *Photosynthetically active radiation measurement*

All PAR measurements were taken to synchronize with canopy spectrometry determinations, with the same target as the spectroscopy measurement, using a LI−191SA line quantum sensor produced by the American LI−COR Company. The instrument's light quantum sensing area was 1 m × 12.7 mm; the sensing wavelength was between 400 and 700 nm; the measured result was the PAR average within the scope of the sensing area; and the output unit was μmol m^{-2} s^{-1}. The measured target included the four fractions of photosynthetically active radiation: photosynthetically active radiation canopy incident (PAR_{ci}), photosynthetically active radiation canopy reflection (PAR_{cr}), photosynthetically active radiation ground incident (PAR_{gi}), and photosynthetically active radiation ground reflection (PAR_{gr}). Top-of-canopy measurements were made by placing the linear quantum sensor about 0.5 m above the canopy, while under-canopy measurements were made at about 0.15 m above the ground. We aimed both ends of the probe's sensing part at the middle position between the rows and aimed the probe's midpoint at the top of the plant row, enabling the horizontal ball to stay on the midpoint of the spirit level thus maintaining the horizontal alignment of the linear quantum sensor.

The (canopy)-absorbed photosynthetically active radiation (APAR) can be estimated by subtracting PAR reflected to the atmosphere and that absorbed by the soil from total incident PAR. Hence, FPAR was calculated using the following (Ridao, Conde, and Minguez 1998):

$$\mathrm{FPAR} = \left[(\mathrm{PAR_{ci}} - \mathrm{PAR_{cr}}) - (\mathrm{PAR_{gi}} - \mathrm{PAR_{gr}})\right] / \mathrm{PAR_{ci}}. \quad (2)$$

2.2.4. Hyperspectral VIs and statistical analysis

In reference to previous studies, based on the spectral characteristics of corn and combined with the physical meaning of spectral index, a total of 54 VIs were considered (Table 1) in relation to FPAR, leaf area index, and chlorophyll (known as an important influence on PAR absorbed by green vegetation) as the independent variables for the establishment of remote-sensing estimation models of corn canopy FPAR. Data from the field experiment in 2009 (76 samples) were used to develop the regression models, and data from the field experiments in 2010 and 2011 (60 samples) were used to evaluate the models.

VI–FPAR relationships were analysed using a variety of regression models – linear, exponential, logarithmic, and quadratic. Models were ranked based on statistically significant ($p < 0.05$ or 0.001) correlation coefficients (r in the case of linear models) and coefficients of determination (R^2 in the case of non-linear models). Finally, by plotting the relation value under the scale 1:1 between estimated and measured FPAR values, the performance of the model was evaluated through the coefficient of determination (R^2) and relative root mean squared error (RRMSE) for the estimation of *in situ*-measured FPAR. The higher the R^2 and the lower the RRMSE, the higher the accuracy of the model to estimate FPAR. RRMSE and estimation accuracy are calculated using Equations (3) and (4), respectively:

$$\mathrm{RRMSE} = \sqrt{\frac{1}{n}\sum_{i=1}^{n}(y_i - \hat{y}_i)^2} \Big/ \frac{1}{n}\sum_{i=1}^{n} y_i, \quad (3)$$

$$\text{Estimation accuracy} = 1 - \mathrm{RRMSE}, \quad (4)$$

where y_i and $\hat{y}_i$ are the measured and predicted values of the corn canopy FPAR, respectively, and n is the number of samples.

3. Results

3.1. Changes in corn canopy FPAR with growth stage

FPAR increases progressively as corn crops progress through different growth stages (Figure 1). An initially large increase in FPAR, by about 36.9%, was observed corresponding to crop development from the jointing stage to the little bell stage. Further increase in FPAR, from the little bell stage to the mid-silking stage, occurred at lower rates (6.12%, 1.95%, 2.61%, and 3.53%, respectively). Until the mid-silking stage, FPAR began to increase and reached its maximum value of 0.86. From the mid-silking to the milk stage, FPAR tended to slow indicating saturation.

3.2. VI–FPAR relationship

Statistically significant correlations between FPAR and VIs are observed in 49 out of 54 VIs considered (Table 2), and these are both positive and negative. Positive correlations between VIs and FPAR were generally stronger than negative. FPAR is most strongly

Table 1. Definition of hyperspectral vegetation indices (VIs) evaluated in the study.

Vegetation index	Abbreviation	Algorithm
Simple ratio 1	SR [787, 765]	R787/R765
Simple ratio 2	SR [415, 710]	R415/R710
Simple ratio 3	SR [415, 695]	R415/R695
Simple ratio 4	SR [750, 705]	R750/R705
Simple ratio 5	SR [900, 680]	R900/R680
Simple ratio 6	SR [801, 670]	R801/R670
Simple ratio 7	SR [672, 550, 708]	R672/(R550 × R708)
Optimized vegetation index 1	VIopt1	R760/R730
Optimized vegetation index 2	VIopt2	100 × (lnR760 – lnR730)
Pigment specific simple ratio 1	PSSR [800, 680]	R800/R680
Pigment specific simple ratio 2	PSSR [800, 635]	R800/R635
Pigment specific simple ratio 3	PSSR [800, 470]	R800/R470
Zarco-Tejada and Miller	ZTM	R750/R710
Red-edge model index	R-M	(R750/R720) – 1
Difference index	DI	R800 – R550
Difference vegetation index	DVI	R800 – R680
Pigment specific normalized difference 1	PSND [800, 635]	(R800 – R635)/(R800 + R635)
Pigment specific normalized difference 2	PSND [800, 470]	(R800 – R470)/(R800 + R470)
Modified simple ratio index 1	mSRI1	(R750 – R445)/(R705 + R445)
Modified simple ratio 2	mSRI2	$(R800/R670 - 1)/\sqrt{R800/R670 + 1}$
Normalized difference index	NDI	(R800 – R680)/(R800 + R680)
Modified normalized difference index	mNDI	(R750 – R705)/(R750 + R705 – 2 × R445)
Plant senescence reflectance index	PSRI	(R680 – R500)/R750
Re-normalized difference vegetation index	RDVI	$(R800 - R670)/\sqrt{R800 + R670}$
Simple ratio pigment index	SRPI	R430/R680
Ratio vegetation index	RVI	(R790 : R810)/(R640 : R660)
Normalized pigments chlorophyll ratio index	NPCI	(R680 – R430)/(R680 + R430)
Normalized phaeophytinization index	NPQI	(R415 – R435)/(R415 + R435)
Structure intensive pigment index	SIPI	(R800 – R445)/(R800 – R680)
MERIS terrestrial chlorophyll index	MTCI	(R750 – R710)/(R710 – R680)

(*Continued*)

Table 1. (*Continued*).

Vegetation index	Abbreviation	Algorithm
Modified chlorophyll absorption in reflectance index	MCARI	$[(R700 - R670) - 0.2 \times (R700 - R550)] \times (R700/R670)$
Green normalized difference vegetation index	GNDVI	$(R800 - R550)/(R800 + R550)$
Modified transformed vegetation index	MTVI	$1.2 \times [1.2 \times (R800 - R550) - 2.5 \times (R670 - R550)]$
Photochemical reflectance index	PRI	$(R531 - R570)/(R530 + R570)$
Transformed vegetation index	TVI	$0.5 \times [120 \times (R750 - R550) - 200 \times (R670 - R550)]$
Temperature condition index	TCI	$1.2 \times (R700 - R550) - 1.5 \times (R670 - R550) \times \sqrt{(R700/R670)}$
Double difference index	DDI	$(R750 - R720) - (R700 - R670)$
Scaled normalized difference vegetation index	NDVI*	$(NDVI - NDVI0)/(NDVIS - NDVI0)$
Modified soil adjusted vegetation index	MSAVI	$[2R800 + 1 - \sqrt{(2R800 + 1)^2 - 8(R800 - R670)}]/2$
Optimal soil adjusted vegetation index	OSAVI	$(1 + 0.16) \times (R800 - R670)/(R800 + R670 + 0.16)$
Transformed chlorophyll absorption in reflectance index	TCARI	$3 \times [(R700 - R670) - 0.2 \times (R700 - R550) \times (R700/R670)]$
Visible atmospherically resistant index	VARI	$(R555 - R680)/(R555 + R680 - R480)$
Wide dynamic range vegetation index	WDRVI	$(\alpha \times Rnir - Rred)/(\alpha \times Rnir + Rred)$, a = 0.05, 0.1, 0.2
Red–green ratio	RGR	$(R612 + R660)/(R510 + R560)$
Normalized difference vegetation index 1	NDVI [760, 708]	$(R760 - R708)/(R760 + R708)$
Normalized difference vegetation index 2	NDVI [800, 600]	$(R800 - R600)/(R800 + R600)$
Normalized difference vegetation index 3	NDVI [780, 550]	$(R780 - R550)/(R780 + R550)$
Normalized difference vegetation index 4	NDVI [800, 700]	$(R800 - R700)/(R800 + R700)$
Normalized difference vegetation index 5	NDVI [900, 680]	$(R900 - R680)/(R900 + R680)$
Ratio between TCI and OSAVI	TCI/OSAVI	TCI/OSAVI
Ratio between MTVI and MSAVI	MTVI/MSAVI	MTVI/MSAVI
Ratio between DDI and MSAVI	DDI/MSAVI	DDI/MSAVI
Ratio between MCARI and OSAVI	MCARI/OSAVI	MCARI/OSAVI
Ratio between TCARI and OSAVI	TCARI/OSAVI	TCARI/OSAVI

Note: R indicates reflectance.

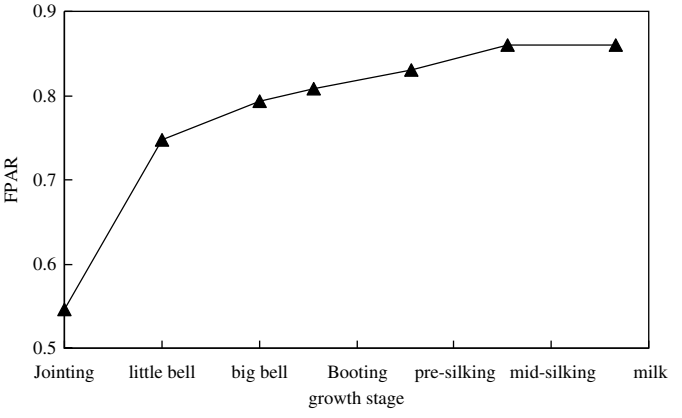

Figure 1. Fraction of photosynthetically active radiation (FPAR) absorbed by corn canopies at different growth stages.

correlated to GNDVI, NDVI*, and NDVI [780, 550] – the correlation coefficients (r) are 0.787, 0.737, and 0.723, respectively. Thus, GNDVI, NDVI*, and NDVI [780, 550] can be identified as three common VIs relatively well correlated to corn canopy FPAR, and these are the most suitable VIs for estimation of FPAR.

Table 2. Linear correlation coefficients (r) for the relationship between the fractions of photosynthetically active radiation (FPAR) absorbed by corn canopies and hyperspectral vegetation indices (VIs).

Vegetation index	r	Vegetation index	r	Vegetation index	r
SR [787, 765]	0.703^{++}	mSRI2	0.634^{++}	MSAVI	0.707^{++}
SR [415, 710]	0.239^{+}	NDI	0.696^{++}	OSAVI	0.697^{++}
SR [415, 695]	-0.329^{++}	mNDI	0.589^{++}	VARI	0.462^{++}
SR [750, 705]	0.488^{++}	PSRI	-0.628^{++}	TCARI	–0.054
SR [900, 680]	0.595^{++}	RDVI	0.655^{++}	WDRVI (a = 0.05)	0.641^{++}
SR [801, 670]	0.583^{++}	SRPI	0.243^{+}	WDRVI (a = 0.1)	0.661^{++}
SR [672, 550, 708]	0.436^{++}	RVI	0.599^{++}	WDRVI (a = 0.2)	0.682^{++}
VIopt1	0.619^{++}	NPCI	-0.252^{+}	RGR	-0.483^{++}
VIopt2	0.649^{++}	NPQI	-0.427^{++}	NDVI [760, 708]	0.701^{++}
PSSR [800, 680]	0.576^{++}	SIPI	-0.647^{++}	NDVI [800, 600]	0.716^{++}
PSSR [800, 635]	0.615^{++}	MTCI	0.418^{++}	NDVI [780, 550]	0.723^{++}
PSSR [800, 470]	0.642^{++}	MCARI	0.238^{+}	NDVI [800, 700]	0.702^{++}
ZTM	0.482^{++}	GNDVI	0.787^{++}	NDVI [900, 680]	0.712^{++}
R–M	0.502^{++}	MTVI	0.567^{++}	TCI/OSAVI	–0.040
DI	0.560^{++}	PRI	0.338^{++}	MTVI/MSAVI	0.524^{++}
DVI	0.574^{++}	TVI	0.327^{++}	DDI/MSAVI	0.233^{+}
PSND [800, 635]	0.704^{++}	TCI	–0.105	MCARI/OSAVI	0.085
PSND [800, 470]	0.709^{++}	DDI	0.332^{++}	TCARI/OSAVI	0.004
mSRI1	0.536^{++}	NDVI*	0.737^{++}	–	–

Note: $^{+}$ and $^{++}$ indicate significant difference at 0.05 and 0.01 probability level, respectively.

3.3. Establishing the FPAR estimation model based on VI

A total of 14 VIs are considered for modelling FPAR based on a threshold of VI–FPAR correlation (i.e. $r > 0.68$ in Table 1). These non-linear FPAR estimation models are best represented as exponential functions and are evaluated using their predictive (R^2) and error statistics (RRMSE) (Table 3). Among these, FPAR has the closest exponential relation with GNDVI, and a closer exponential relation with NDVI* and NDVI [780, 550], and the models based on GNDVI, NDVI*, and NDVI [780, 550] are capable of estimating FPAR with R^2 of 0.647, 0.594, and 0.561, respectively, with RRMSE of 0.179, 0.216, and 0.237, respectively, and with estimation accuracy of 82.1%, 78.4%, and 76.3%, respectively. Furthermore, according to comparisons of R^2, RRMSE, and estimation accuracy, it is more suitable to estimate corn canopy FPAR by GNDVI and NDVI* (Figure 2) than by NDVI [780, 550].

3.4. Saturation analysis of VIs

All three VIs in Figure 3 – GNDVI, NDVI*, and NDVI [780, 550] – with the strongest relationship to FPAR increase progressively with increase in FPAR up to about 0.75. Beyond this point, GNDVI and NDVI [780, 550] values start levelling off, at 0.72 and 0.83, respectively, which is known as saturation. On the other hand, NDVI* displays a different tendency (i.e. decrease beyond FPAR values of about 0.75). Using this information, a reliable FPAR model can be constructed such that GNDVI is the predictor before the onset of saturation (FPAR ≤ 0.75), while NDVI* is the predictor beyond the saturation point (FPAR > 0.75), which will effectively address the issue of VI saturation.

Based on the aforementioned research results, the segmented hyperspectral estimation model of FPAR was built according to the range of FPAR values in Figure 4. Namely, if FPAR ≤ 0.75, GNDVI should be used to estimate FPAR and the estimation model is $y = 0.1825e^{1.8588x}$, $R^2 = 0.836$ ($p < 0.01$); if FPAR > 0.75, NDVI* should be used to estimate FPAR and the estimation model is $y = -0.6312x + 1.0128$, $R^2 = 0.772$ ($p < 0.01$).

Table 3. Quantitative relationships between the fraction of photosynthetically active radiation absorbed (FPAR; y) by corn canopies and hyperspectral vegetation indices (x).

Hyperspectral vegetation index	Model	R^2	RRMSE
SR [787, 765]	$y = 0.0167e3.2516x$	0.547^{++}	0.258
PSND [800, 635]	$y = 0.1781e1.8864x$	0.548^{++}	0.253
PSND [800, 470]	$y = 0.0445e3.3063x$	0.551^{++}	0.249
NDI	$y = 0.1922e1.7272x$	0.536^{++}	0.274
GNDVI	$y = 0.1545e2.2646x$	0.647^{++}	0.179
NDVI*	$y = 0.4787e1.5783x$	0.594^{++}	0.216
MSAVI	$y = 0.0218e2.5852x$	0.551^{++}	0.251
OSAVI	$y = 0.1903e1.5191x$	0.538^{++}	0.274
WDRVI0.2	$y = 0.6134e0.8333x$	0.503^{++}	0.293
NDVI [760, 708]	$y = 0.2544e1.4962x$	0.541^{++}	0.264
NDVI [800, 600]	$y = 0.1632e2.0695x$	0.557^{++}	0.246
NDVI [780, 550]	$y = 0.1172e2.5377x$	0.561^{++}	0.237
NDVI [800, 700]	$y = 0.1976e1.6823x$	0.547^{++}	0.259
NDIV [900, 680]	$y = 0.1839e1.7698x$	0.552^{++}	0.249

Note: $^{++}$ indicates significant difference at 0.01 probability level.

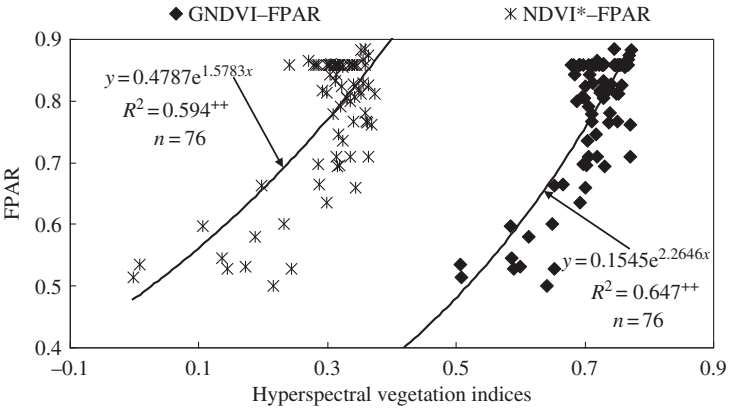

Figure 2. GDNVI–FPAR and NDVI*–FPAR relationships for corn canopies.
Note: $^{++}$ indicates significant difference at 0.01 probability level.

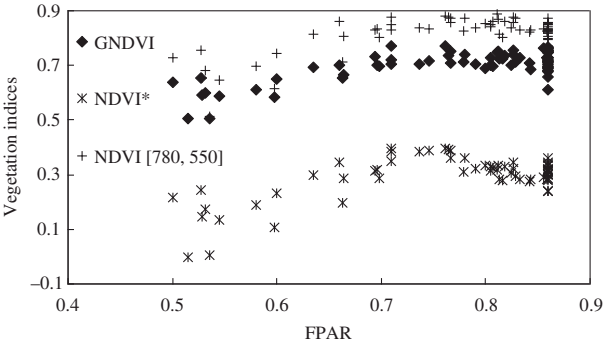

Figure 3. Changes in GNDVI, NDVI*, and NDVI [780, 550] with the fraction of photosynthetically active radiation (FPAR) absorbed by corn canopy (n = 76).

3.5. *Evaluation of VI-based FPAR model*

A total of 60 samples from the experiments in 2010 and 2011 were used to test the hyperspectral VI-based estimation model of FPAR mentioned above (see Section 3.4). The estimated and measured FPAR cross-resistance almost converged with the 1:1 relation line shown in Figure 5 for comparison. At low FPAR values, estimated value may be underestimated. As FPAR increases, estimated values are closer to the measured values. The R^2, RRMSE, and estimation accuracy values of the segmented FPAR model are 0.782, 0.093, and 90.7%, respectively. Compared with the estimation models based on only GNDVI, NDVI*, and NDVI [780, 550] in Table 3, the estimation accuracy values of the segmented FPAR model in the different ranges of FPAR increased by 8.6%, 12.3%, and 14.4%, respectively. In conclusion, the segmented model based on GNDVI and NDVI* used to estimate FPAR can not only improve the estimation accuracy, but also solve the saturation problems that occurred with GNDVI and NDVI [780, 550].

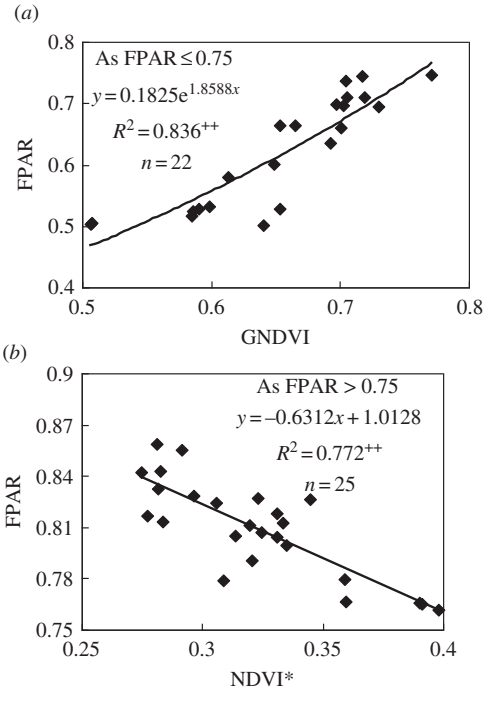

Figure 4. Hyperspectral VI-based estimation models of fraction of photosynthetically active radiation (FPAR) absorbed by corn canopies. Shown here are (*a*) GNDVI–FPAR model (FPAR ≤ 0.75) and (*b*) NDVI*–FPAR model (FPAR > 0.75).
Note: $^{++}$ indicates significant difference at 0.01 probability level.

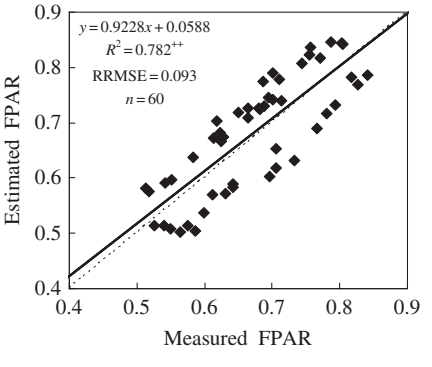

Figure 5. Evaluation of the estimation capability of the segmented model for the fraction of photosynthetically active radiation (FPAR) absorbed by the corn canopy.
Note: $^{++}$ indicates significant difference at 0.01 probability level. The solid and dashed lines represent the actual and 1:1 relations between estimated and measured values of FPAR, respectively.

4. Discussion and conclusions

FPAR is primarily controlled by ground cover and leaf area (Myneni and Williams 1994). Before the little bell stage, FPAR increases significantly (Figure 1), which is characterized by strong absorption of incoming PAR as corn crops grow vigorously and enhance leaf area,

driven by nitrogen fertilization. This is followed by a lower rate of crop growth (and leaf area expansion), which is captured by the lower rate of FPAR increase. According to the agronomic principles for corn, although the research lacked FPAR data after the milk stage, it is still possible to conclude that leaves started to turn yellow and gradually litter as the growth period passed, and FPAR declined due to the combination of corn's photosynthetic physiological characteristics. Until the fully ripe stage, FPAR was close to 0 because leaves withered and died and thus became unable to absorb light energy and no longer accumulated dry matter.

Significant efforts are presently focused on the use of VIs in general, and NDVI in particular, for estimating vegetation canopy FPAR. Furthermore, many studies indicate that VIs are better correlated to FPAR than the reflectance in single wavebands (Epiphanio and Huete 1995; Ridao, Conde, and Minguez 1998; Fensholt, Sandholt, and Rasmussen 2004; Olofsson and Eklundh 2007; Yang et al. 2007; Chiesi et al. 2011), which could plausibly be explained by the fact that VIs can minimize the influence of atmospheric scattering and soil background and enhance the information of the sensitive wavebands (Chen 1996a, 1996b; Huete et al. 2002). Similarly, this study found FPAR to be strongly correlated to the majority of VIs (49 out of 54), with GNDVI, NDVI*, and NDVI [780, 550] being the best performing. This result is helpful in providing an important technique for the establishment of perfect corn photosynthetic groups, the improvement of sunlight energy efficiency, and the implementation of cultivation control.

As compared with previous studies with NDVI, GNDVI and NDVI* for estimating FPAR showed lower RRMSE and higher estimation accuracy than those proposed for NDVI in several studies (Myneni and Williams 1994; Bastiaanssen and Ali 2003; Yang et al. 2007; Chiesi et al. 2011).

Vegetation indices such as NDVI are often plagued with saturation in areas of high biomass (Myneni and Williams 1994; Olofsson and Eklundh 2007; Yang et al. 2007; Samanta et al. 2012), which is a major disadvantage for VI–FPAR models. We addressed this issue by exploiting the differences in sensitivity of different VIs to FPAR (i.e. when FPAR is greater than 0.75, GNDVI and NDVI (780, 550) tend to level off, but NDVI* shows a decline). Accordingly, our proposed piecewise FPAR model uses GNDVI (FPAR $\leq$ 0.75), or NDVI* (FPAR > 0.75) as the regress. Given that VIs can be estimated consistently from both field-based spectral data, as used here, and satellite data, this model can also be based on either data source. This makes our model a useful resource not only for current satellite data, but also for data from future satellite sensors (such as HysPIRI).

Future research should focus on evaluating the performance of the proposed model over corn crops grown under a variety of conditions, different corn varieties, and other crop types. This will help in refining the model as a useful tool for informing crop management practices. Efforts should also be made to test this model with data from different sources – field-based spectral measurements, as well as current and future satellite data.

Funding

Financial assistance for this research was provided by the National Natural Science Foundation of China [grant number 41271415], [grant number 40801122]; and a project funded by the Priority Academic Programme Development (PAPD) of Jiangsu Higher Education Institutions.

References

Bastiaanssen, W. G. M., and S. Ali. 2003. "A New Crop Yield Forecasting Model Based on Satellite Measurements Applied Across the Indus Basin, Pakistan." *Agriculture, Ecosystem and Environment* 94: 321–340.

Chen, J. 1996a. "Canopy Architecture and Remote Sensing of the Fraction of Photosynthetically Active Radiation in Boreal Conifer Stands." *IEEE Transactions on Geoscience and Remote Sensing* 34: 1353–1368.

Chen, J. 1996b. "Evaluation of Vegetation Indices and a Modified Simple Ratio for Boreal Applications." *Canadian Journal of Remote Sensing* 22: 229–242.

Chiesi, M., L. Fibbi, L. Genesio, B. Gioli, R. Magno, F. Maselli, M. Moriondo, and F. P. Vaccari. 2011. "Integration of Ground and Satellite Data to Model Mediterranean Forest Processes." *International Journal of Applied Earth Observation and Geoinformation* 13: 504–515.

Coops, N. C., J. S. Michaud, M. E. Andrew, and M. A. Wulder. 2011. "Comparison of a Regional-Level Habitat Index Derived from MERIS and MODIS Estimates of Canopy-Absorbed Photosynthetically Active Radiation." *Remote Sensing Letters* 2: 327–336.

Daughtry, C. S., K. P. Gallo, S. N. Goward, S. D. Prince, and W. P. Kustas. 1992. "Spectral Estimates of Absorbed Radiation and Phytomass Production in Corn and Soybean Canopies." *Remote Sensing of Environment* 39: 141–152.

Eduardo, R., R. C. Jose, and M. I. Minguez. 1998. "Estimating FPAR from Nine Vegetation Indices for Irrigated and Non-Irrigated Faba Bean and Semi Leafless Pea Canopies." *Remote Sensing of Environment* 66: 87–100.

Epiphanio, J. C. N., and A. R. Huete. 1995. "Dependence of NDVI and SAVI on Sunhemor Geometry and Its Effect on *FPAR* Relationships in Alfalfa." *Remote Sensing of Environment* 51: 351–360.

Fensholt, R., I. Sandholt, and M. Rasmussen. 2004. "Evaluation of MODIS LAI, *FPAR* and the Relation Between *FPAR* and NDVI in a Semi-Arid Environment Using In Situ Measurements." *Remote Sensing of Environment* 91: 490–507.

Friedl, M. A., F. W. Davis, J. Michaelsen, and M. A. Moritz. 1995. "Scaling and Uncertainty in the Relationship Between the NDVI and Land Surface Biophysical Variables: An Analysis Using a Scene Simulation Model and Data from FIFE." *Remote Sensing of Environment* 54: 233–246.

Gobron, N., B. Pinty, O. Aussedat, J. Chen, W. B. Cohen, R. Fensholt, V. Gond, K. F. Hummerich, T. Lavergne, F. Mélin, J. L. Privette, I. Sandholt, M. Taberner, D. P. Turner, M. M. Verstraete, and J. L. Widlowski. 2006. "Evaluation of Fraction of Absorbed Photosynthetically Active Radiation Products for Different Canopy Radiation Transfer Regimes: Methodology and Results Using Joint Research Center Products Derived from SeaWiFS Against Ground-Based Estimations." *Journal of Geophysical Research* 111: 1–15.

Goward, S., and K. Huemmrich. 1992. "Vegetation Canopy PAR Absorptance and the Normalized Difference Vegetation Index: An Assessment Using the SAIL Model." *Remote Sensing of Environment* 39: 119–140.

Goward, S., R. Waring, D. Dye, and J. Yang. 1994. "Ecological Remote Sensing at OTTER: Satellite Macroscale Observations." *Ecological Application* 4: 322–343.

Hall, F., K. Huemmrich, S. J. Goetz, P. Sellers, and J. Nickeson. 1992. "Satellite Remote Sensing of Surface Energy Balance: Successes, Failures and Issues in FIFE." *Journal of Geophysical Research* 97: 19061–19089.

Huete, A., K. Didan, T. Miura, E. Rodriguez, X. Gao, and L. Ferreira. 2002. "Overview of the Radiometric and Biophysical Performance of the MODIS Vegetation Indices." *Remote Sensing of Environment* 83: 195–213.

Ma, J. Y., J. M. Liu, S. K. Li, H. Liang, C. Y. Jiang, and B. Z. Wang. 2007. "Study on the Features of the Photosynthetic Active Radiation (PAR) with Experimentations and Measurements." [In Chinese.] *Journal of Natural Resource* 22: 673–682.

Moreau, L., and Z. Q. Li. 1996. "A New Approach for Remote Sensing of Canopy Absorbed Photosynthetically Active Radiation. II: Proportion of Canopy Absorption." *Remote Sensing of Environment* 55: 192–204.

Myneni, R., and D. Williams. 1994. "On the Relationship Between FPAR and NDVI." *Remote Sensing of Environment* 49: 200–211.

Olofsson, P., and L. Eklundh. 2007. "Estimation of Absorbed PAR Across Scandinavia from Satellite Measurements. Part II: Modeling and Evaluating the Fractional Absorption." *Remote Sensing of Environment* 110: 240–251.

Ren, J. Q., Z. X. Chen, H. J. Tang, and R. X. Shi. 2006. "Study on Regional Winter Wheat Yield Estimation Based on the Vegetation Net Primary Production Model." [In Chinese.] *Transactions of Chinese Society of Agricultural Engineering* 22: 111–117.

Ridao, E., J. R. Conde, and M. I. Minguez. 1998. "Estimating FPAR from Nine Vegetation Indices for Irrigated and Non-Irrigated Faba Bean and Semileafless Pea Canopies." *Remote Sensing of Environment* 66: 87–100.

Roujean, J. L., and F. M. Breon. 1995. "Estimating PAR Absorbed by Vegetation from Bi-Directional Reflectance Measurements." *Remote Sensing of Environment* 51: 375–384.

Ruimy, A., and B. Saugier. 1994. "Methodology for the Estimation of Terrestrial Net Primary Production from Remotely Sensed Data." *Journal of Geophysical Research* 97: 18515–18521.

Samanta, A., Y. Knyazikhin, L. Xu, R. E. Dickinson, R. Fu, M. H. Costa, S. S. Saatchi, R. R. Nemani, and R. B. Myneni. 2012. "Seasonal Changes in Leaf Area of Amazon Forests from Leaf Flushing and Abscission." *Journal of Geophysical Research* 117: G01015. doi:10.1029/2011JG0018.

Sellers, P. J., R. E. Dickinson, D. A. Randall, A. K. Betts, F. G. Hall, J. A. Berry, G. J. Collatz, A. S. Denning, H. A. Mooney, C. A. Nobre, N. Sato, C. B. Field, and A. Henderson-Sellers. 1997. "Modeling the Exchanges of Energy, Water and Carbon Between Continents and the Atmosphere." *Science* 275: 502–509.

Senna, M., M. Costa, and Y. Shimabukuro. 2005. "Fraction of Photosynthetically Active Radiation Absorbed by Amazon Tropical Forest: A Comparison of Field Measurements, Modeling, and Remote Sensing." *Journal of Geophysical Research* 110: g01008. doi:10.1029/2004JG005.

Smith, K. L., M. D. Steven, and J. J. Colls. 2004. "Use of Hyperspectral Derivative Ratios in the Red-Edge Region to Identify Plant Stress Responses to Gas Leaks." *Remote Sensing of Environment* 92: 207–217.

Turner, D., W. Ritts, W. Cohen, T. Maeirsperger, S. Gower, A. Kirschbaum, S. Running, M. S. Zhao, S. Wofsy, A. Dunn, B. Law, J. Campbell, W. Oechel, H. Kwon, T. Meyers, E. Small, S. Kurc, and J. Gamon. 2005. "Site-Level Evaluation of Satellite-Based Global Terrestrial Gross Primary Production and Net Primary Production Monitoring." *Global Change Biology* 11: 666–684.

Wu, B. F., Y. Zeng, and J. L. Huang. 2004. "Overview of LAI/FPAR Retrieval from Remotely Sensed Data." [In Chinese.] *Advanced Earth Science* 19: 585–590.

Wu, C. Y., X. Z. Han, J. S. Ni, Z. Niu, and W. J. Huang. 2010. "Estimation of Gross Primary Production in Wheat from In Situ Measurements." *International Journal of Applied Earth Observation and Geoinformation* 12: 183–189.

Yang, F., B. Zhang, K. S. Song, Z. M. Wang, J. C. You, D. W. Liu, and J. P. Xu. 2007. "Hyperspectral Estimation of Corn Fraction of Photosynthetically Active Radiation." *Agricultural Sciences in China* 6: 1173–1181.

Zhao, P. J., D. W. Wang, C. Y. Huang, and Q. J. Ma. 2009. "Estimating of Cotton Canopy Fraction of Photosynthetically Active Radiation and Leaf Area Index Based on Hyperspectral Remote Sensing Data." [In Chinese.] *Cotton Science* 21: 388–393.